Universiteit Utrecht

Opleiding Natuur- en Sterrenkunde

Simulating pathways and beaching effects of plastic originating from the Dutch coast

BACHELOR THESIS

Jeroen Paul van Rijn

Supervisor:

Dr. Erik VAN SEBILLE
Institute for Marine and Atmospheric Research

July 23, 2018

Abstract

In this thesis, we look at the pathways of plastic originating from the Dutch shore and are interested in where this plastic ends up. We use global buoy trajectory observations and model data to construct transition matrices to model the ocean at the surface layer. With these transition matrices, we simulate a plastic tracer distribution over time by means of a Markov model. We also construct a model to simulate beaching effects based on the proximity of tracer to a coast and investigate its effects. It was found that most plastic released from the Dutch coast moves northwards towards the Barents Sea and remains circulating in the gyre formed there, while a considerable portion of plastic moves towards and remains in circulation east of Denmark. When beaching is taken into account, we see that the highest concentration of plastic washed ashore accumulates on the (east) Danish shore, while considerable amounts end up on the Norwegian and Dutch coasts as well. It was also found that very little plastic washes up on the UK coast.

Since there is little empirical data on the scale of beaching, we vary the intensity of our beaching model to explore how this affects the results. To grasp these variations will allow for easier retroactive calibration of our model as more data on beaching becomes available. It was found that increasing the scaling factor in our model increased the total amount of beaching and showed a slight proportional beaching increase for areas closer to the point of origin of the plastic.

Contents

1   Introduction

Plastic ending up in and polluting the oceans is becoming increasingly problematic. With increasing plastic production due to industrialization and rise in consumerism, influxes of plastic into the ocean have generally been increasing for many years. Since plastic does not biodegrade, any plastic that does not wash ashore or is fished out of the ocean will remain in circulation almost indefinitely. The impacts on the environment due to this are far-reaching. Marine life can get trapped in plastics or mistake plastics for food, leading to serious health issues [4]. Besides impacts on the environment, plastics in the ocean have socio-economic consequences as well. Pictures of beaches full of washed-up plastic have become ubiquitous in recent years and heavily polluted beaches have seen their tourism activity dropped, impacting livelihoods of the local populace [17]. Whereas the problem has been part of the public conscience for many years, only recently have considerable efforts been made by politics and business to mitigate the influx of plastic in the oceans. As efforts to reduce influxes are gaining traction, likewise some initiatives to remove plastic from the ocean are starting up and receiving popular media attention.

In order to alleviate the problem of plastic that has reached the ocean, it is important to have a good grasp of the pathways followed by plastic debris. Previous studies have determined that most marine debris ends up in one of the five major ocean garbage patches in a few years after their release and remain there for decades [16] [5]. This is largely due to convergence of debris towards the five major gyres in the ocean, which results in accumulation of debris in patches. The gyres are the net result of a combination of most large scale ocean movements in the surface layer. The Ekman transport resulting from trade winds and westerlies move water towards the center of the oceans to create a raised sea surface, which in turn creates a pressure gradient outwards of these centers. The resulting gradient finds an equilibrium with the Coriolis force and this results in a stable cyclical geostrophic current around these centers in which most debris remains once they reach this current [2]. These gyres are a strong contributing factor to debris movements, although previous studies suggest there is more movement between these patches on the centennial scale than has previously been appreciated [16].

Most of these studies have been set up to look at debris pathways on a global scale, but due to the complexity and turbulent nature of ocean currents, local variance can play a significant role. Some studies have been done before for other regions, but none have been performed so far for the Dutch coast. Furthermore, mostly due to lack of empirical data, most previous studies have not taken local effects such as beaching (i.e. washing ashore of debris) into account.

In this study, we will create a model of the ocean currents by looking at observed buoy trajectories and data created by resolving eddy motions. We simulate a tracer dispersing according to this model, in order to simulate plastic starting from the Dutch coast. We consider the plastic pathways and destinations on a decennial timescale. We will also take into account the effect that beaching has on these pathways and briefly discuss the different effects on these results due to release time, model resolution and release location along the

Dutch coast.

Our research question is: "Where does floating plastic released in the ocean from the Dutch coast end up, and which contribution does beaching have to its pathways?" We expect most plastic to reach and remain in one of the previously mentioned gyres and we expect a significant amount of plastic to wash up on shore, since the North Sea is narrow and plastic will therefore likely wash ashore close to its origin location.

2   Method

2.1   Observational drifter data and model data

In order to appropriately model the ocean surface currents over time, we make use of observed buoy trajectories from drifters deployed since February 1979 until January 2013. These buoy trajectories are provided by the NOAA's Global Drifter Program, which has deployed approximately 1000 drifters per year with a mean lifetime of 450 days for a period of 34 years [6]. Every month since 1993, there have been more than 600 drifting buoys in the ocean providing measurements for this dataset [11]. Since these buoys float around on the ocean surface, they are appropriate for modelling the ocean surface flows and are therefore applicable to studying the pathways of floating debris. The buoys were released with a 15m drogue, which serves to average the flow in the upper layer of the ocean, which mitigates wind effects at the surface.

While 52% of buoys lose their drogue over their lifetime and are therefore more prone to wind forcing and wind drift, we combine the data from drogued and non-drogued buoys. The reason we do not differentiate is that this increases our sample size, is more representative of vertical plastic distribution, which is a mix of positively and near-neutrally buoyant particles. Furthermore, research has shown that both types of buoys largely aggregate in the same regions [16] [8]. These drifter buoys provide us with a GPS coordinates for their location for every buoy every 6 hours. Due to the number of buoys and the large timescale on which they were released, this data covers the ocean quite well: over 85% of $1° \times 1°$ areas have at least 100 data points in them [15].

However, as can be seen in figure 1a, one of the areas with virtually no coverage is the North Sea, likely because of drifting buoys running aground due to the shallow depth of the sea. Since the Dutch coast is exclusively along the North Sea, this is obviously a problem for our purposes here. In order to overcome this, additional model data is used similarly to the van Sebille paper [14]. The model has been shown to accurately reproduce the circulation in many areas of the ocean [7]. This model data was created with a model dataset based on OGCM (Ocean general circulation model) for the Earth Simulator data (OFES for short), that was used to resolve eddy ocean motions. This model has a horizontal resolution of $0.1°$ and 54 vertical levels. In total, 455,236 particles were simulated in the velocity fields provided by the model over a period of one year using the Connectivity Modeling System version 1.1 [14]. Coverage in the European area for both datasets is plotted in figure 1.

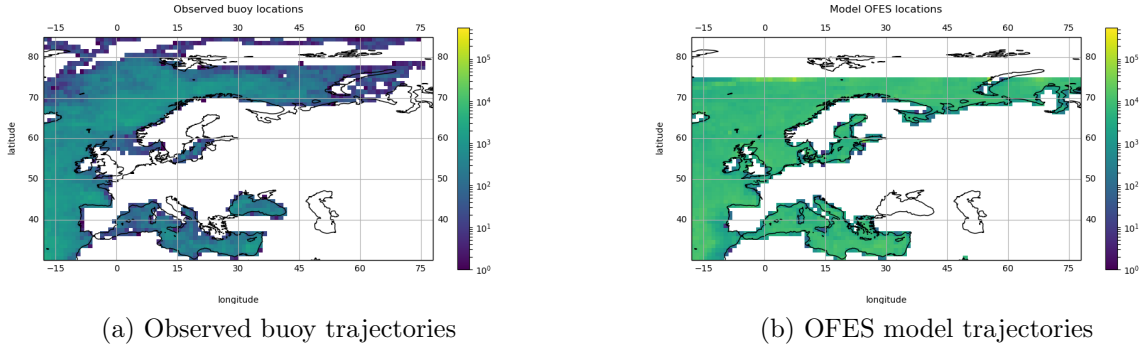(a) Observed buoy trajectories   (b) OFES model trajectories

Figure 1: Comparison of the observed buoy coverage and OFES model data coverage used to construct transition matrices. Color scale denotes amount of datapoints per grid cell and is plotted logarithmically.

2.2   Transition matrix approach

Our next step is to use these observational data and model data predictively, using a transition matrix method (also known as a Markov model). This method is a way of modeling for the evolution of a tracer distribution v in time by iteratively solving

$$\vec{v}_{t+\tau} = \vec{v}_t P_m, \tag{1}$$

where t is time, $\vec{v}$ is a vector with tracer concentrations for discretized space and P_m is the transition matrix for the probability of $\vec{v}$'s evolution after one timestep of size τ, with m as the index for each timestep. By solving this equation iteratively for a multiple of timesteps τ, the advection of tracer in the ocean over time can be modelled. In order to do so, we must construct transition matrices P_m that predict the dispersion of tracer distributions. We assume oceans have negligible interannual variation but do have interseasonal variation, so the probability matrices are defined within a one year period and repeatedly used for simulations spanning multiple years.

To construct transition matrices from our aforementioned data, we first construct crossing matrices by tallying all movements our particles make. We define a two-dimensional grid to cover the entire world area with a fixed dx in degrees longitude and latitude for each grid cell, resulting in a total of grid cells $n_c = (\frac{360}{dx} + 1) * (\frac{180}{dx} + 1)$. Furthermore, we decide upon a timestep $\tau < 1$ year and create a total of n_t crossing matrices C_m, where n_t is the amount of timesteps τ in one year and $m \in [1, n_t]$ denoting the timestep index in one year. Since we assume no differences from one year to another, all crossings over the 34 year period buoys were observed are counted in the same n_t crossing matrices corresponding to one year. The dimensions of these n_t matrices are $n_c \times n_c$, where every column i denotes an origin location and every row j denotes a destination for a particle that left origin i. For each of our datapoints (which were recorded at an interval of $dt = 6$hrs), we determine one location i at time t and the location j of that same particle at time $t + \tau$ on the model grid, and increment entry $C_{m_{ij}}$ with 1 for timestep m in which t falls. For example, for $\tau = 1$ month, we consider a particle at June 5 12a.m.: if it is in grid cell $i = 30$ at that moment and is in $j = 40$ on

July 5 12a.m., then $C_{6_{30,40}}$ gets incremented by 1.

For our purposes and our dataset, a timestep τ of 60 days is reasonable. A timestep of more than 90 days would mean seasonal variability are not accounted for and a timestep smaller than 60 days would mean some regions of the ocean would have inadequate movement, causing plastic to get stuck in some places artificially due to limitations of the model [16]. Also, smaller timesteps correspond to larger errors in results due to artificial dispersion in transition matrix modeling, which is further elaborated on in the Discussion section of this thesis [9]. Our total number of crossing matrices will therefore be 6, corresponding to the months January-February, March-April, ... , November-December.

Since we prefer to rely on observational data instead of model data where we can, we use a weighing factor $w = 10$ for all observed buoy crossings compared to the model data, such that $C_m = C_{m_{buoy}} * w + C_{m_{model}}$. This ensures the contribution of observational buoy data is of the same order of magnitude as our model data in areas where both are available [14].

After constructing these crossing matrices, we normalize each row per origin location, such that

$$P_{m_{i,j}} = \frac{C_{m_{i,j}}}{\sum_j C_{m_{i,j}}}, \tag{2}$$

resulting in a transition matrix that corresponds to the probability for a tracer to move from any location i to any location j after one timestep.

Some alterations to the transition matrices are made. For instance, some grid cells have buoy movement in some timesteps, but not in all. For these locations i, $P_{m_{i,j}} = 0$ for all j in timesteps where there is no movement, and when solving equation 1 for these locations, tracer that reached these cells in previous timesteps will be deleted. To solve this, we artificially set $P_{m_{i,i}} = 1$ for these locations, i.e. the chance for tracer in this grid cell to stay in the same grid cell for this timestep is 1. Another alteration was made to grid cells that have at least one buoy datapoint moving in, but not one moving out. Due to the nature of our model, these grid cells would act as artificial sinks for our tracer, even though this is more likely the result of inadequate data coverage for these grid cells than physical reality. To solve this, we take $P_{m_{i,j}}$ for these grid cells from the timestep they move into these grid cells and set $P_{m+1_{j,i}}$ equal to $P_{m_{i,j}}$, effectively functioning as a reflective boundary condition. After these alterations, the transition matrices are renormalized.

All cells that have no movement at all are considered points on land. The total amount of cells that have movement and are considered ocean cells is $N = 126,688$, out of a total of $N = 202,601$ grid cells for model resolution $dx = 0.5°$.

2.3   Beaching model

In the previous section, we explored a transition matrix method for a system in which all tracer is conserved over time. However, plastic concentrations floating in the ocean are not, since it is not a closed system. A more accurate representation would be
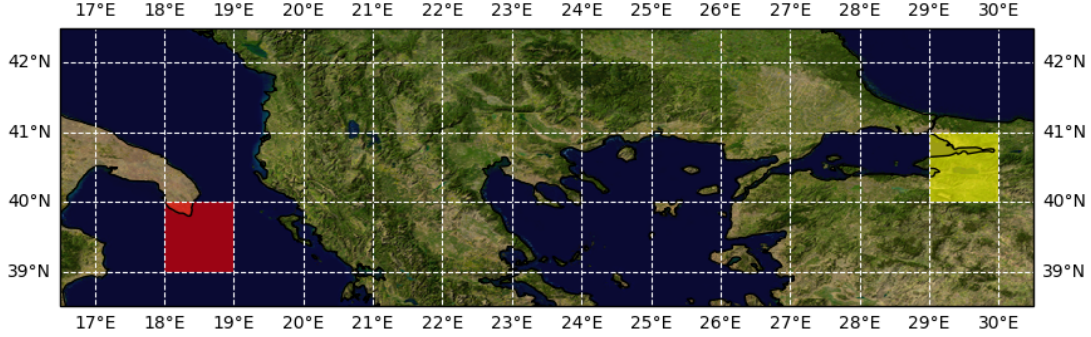
Figure 2: Two cell examples around Greece on the $dx = 1°$ scale. Both are considered ocean cells despite big differences in layout. The yellow cell consists of 90% land and the red cell consists of 5% land.

$$\vec{v}_{t+\tau} = \vec{v}_t P_m + \vec{S} \qquad (3)$$

where $\vec{S}$ is the sources and sinks of $\vec{v}$ per timestep, such as plastic inputs, sinking of plastic to the bottom of the ocean due to biofouling and beaching. Previous studies used a similar way of representing the sources and sinks [6] [8]. One of the relevant sinks involved in plastic distribution that is currently insufficiently understood (largely due to lack of empirical data), is the amount of plastic leaving the ocean by washing ashore, also referred to as beaching.

In order to make an estimate of how much of our circulating tracer ends up on a shore, we look at how much tracer travels near a shore. One coarse method is comparing one grid cell with tracer in it to its adjacent cells and setting the chance of the tracer in a grid cell ending on shore proportional to the amount of adjacent grid cells that are land cells. However, in our model, every grid cell that has any buoy crossing it at some point is defined as an ocean cell, since tracer can reach and leave some location within that cell. As a result, what qualifies as an ocean cell varies wildly between cells. For instance, in figure 2 we see two examples of grid cells that are defined as ocean cells because at least some particle moved through it, but vary in amount of land in the cell.

A better method of approaching this problem, is to make beaching proportional to the amount of land that is in an ocean cell. The more land that is in a grid cell, the higher the chance is that tracer within this grid cell will travel close enough to the shore to end up on land. To determine the amount of land in each grid cell, we use elevation data to determine the fraction of land in each grid cell on a smaller spatial scale than our transitional matrix

model is. The data is provided by NASA and is itself based on the GTOPO30 dataset by the U.S. Geological Survey, which is a topographical dataset with a horizontal resolution of 30 arcseconds (0.00833°) [10] [13]. The elevation data has height values $0 < h < 8848m$ for land points and $h = 99999m$ for ocean values, making an easy cut-off point to distinguish between the land and ocean for our purposes. This elevation data has a spatial resolution of $dx = 0.1°$, which is the result of binning the original 30 arcseconds resolution input data from the U.S. Geological Survey. We in turn bin this data for every larger grid cell in the tracer model we use. The resulting fraction b of land and ocean for every grid cell is determined as

$$b_i = \frac{n_{landcells}}{n_{totalcells}}$$

for all cells with elevation data in every model grid cell i, resulting in values $0 \leq b \leq 1$. Our resulting vector $\vec{b}$ has the same dimensions as $\vec{v}$.

When comparing this beach model to a map of the area, we see that the model represents the coastlines appropriately. On open ocean and inland areas, b is 0 and 1 respectively. The value of b on coastlines is proportional to the size of the land mass in the grid cell (see figure 3).

To use this beaching model, we integrate the following equation for each timestep:

$$\vec{v}_{t+\tau} = \vec{v}_t P_m + \vec{S} = \vec{v}_t P_m * (1 - s * \vec{b}) \tag{4}$$

where s is a fitted scaling factor to scale for the intensity of beaching effects in a cell that can be determined experimentally. Describing the effects of various scaling factors s will be one of the aims of this research. Finding the different effects on our model with different scaling factors will make calibration of the model possible as more empirical data on beaching becomes available. This method is similar to the captEff used in the study by Sherman et al. [12].

2.4 Technical specifications

When running the simulation in time, some floating point rounding errors arise in $\vec{v}$ per iteration due to the large number of model cells and the small concentrations in some cells. Therefore, in order to assure tracer conservation, $\vec{v}$ is renormalized after every iteration. We use Python 2.7.5, Numpy 1.13.3 and Scipy 0.19.1 on the Gemini cluster of Utrecht University for generating our simulation data and Python 3.6.3, Numpy 1.14.2, Cartopy 0.15.1 and Matplotlib 2.1.2 for visualizing our data. All floating points values are of numpy.double precision. All scripts used to generate simulation data can be found on the GitHub repository `https://github.com/OceanParcels/transition_matrices_plasticadrift`.

3 Results

3.1 Location of release on Dutch coast

While the Netherlands is a fairly small country, it does have a relatively large coastline. This raises the question whether differences in release location on the Dutch coast is a relevant
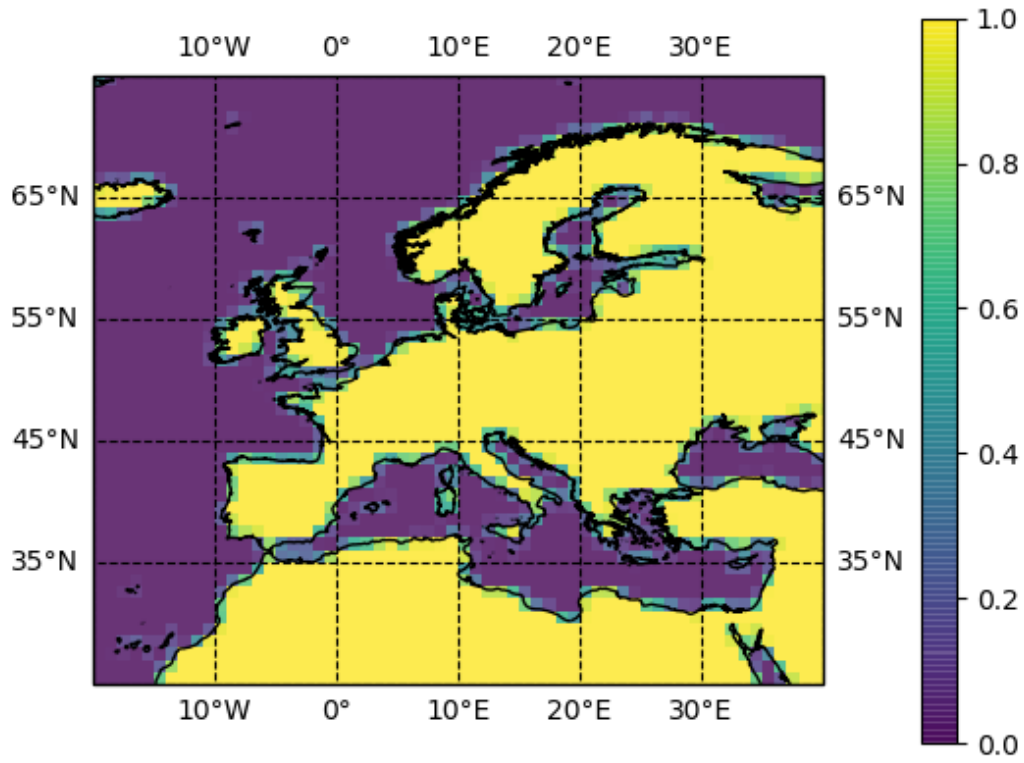
Figure 3: Plot of beaching fraction b per model grid cells around Europe. As expected, $b = 0$ for open sea cells, $b = 1$ for inward land cells and in between those values for coastlines

Figure 4: Locations from which plastic is released on the $dx = 1°$ scale
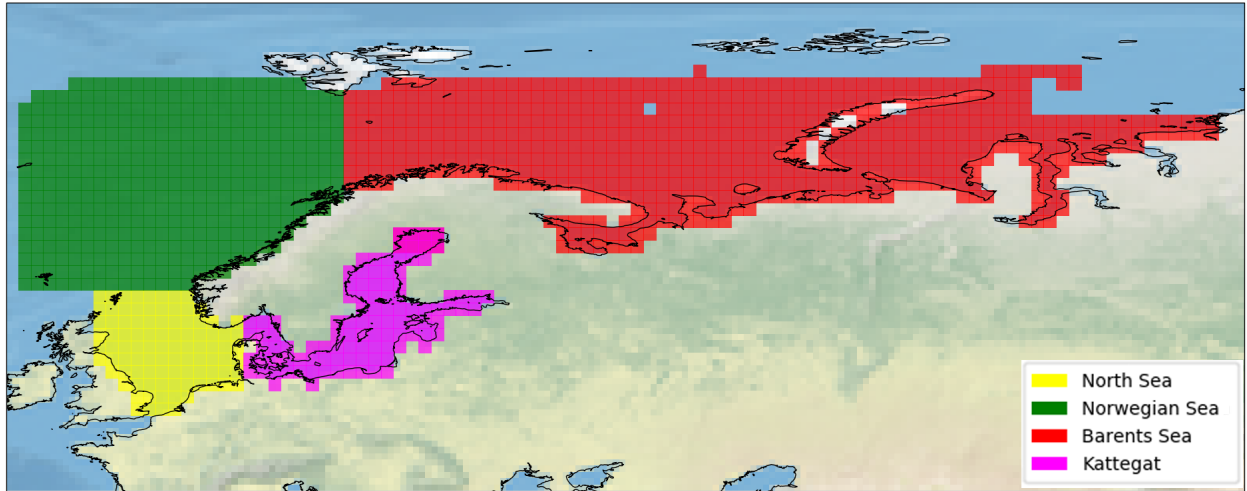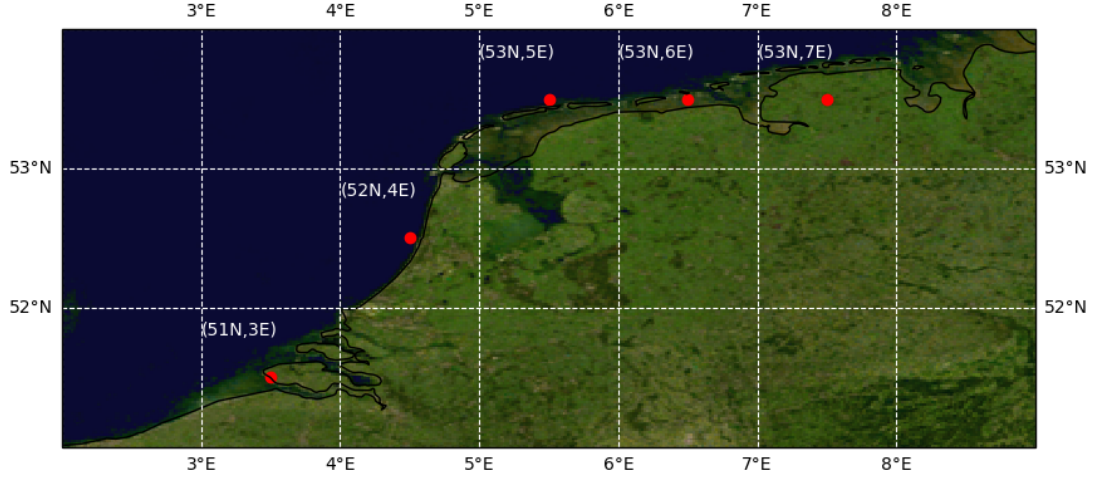

Figure 5: Size and location of the areas as defined in other graphs. Note that area "Kattegat" includes the Baltic Sea, but the name is omitted from the legend since no plastic actually went into the Baltic Sea. The "Barents Sea" extends into the Kara Sea as well, but most of the plastic does not travel this far east. The names are shortened for readability in the graphs.
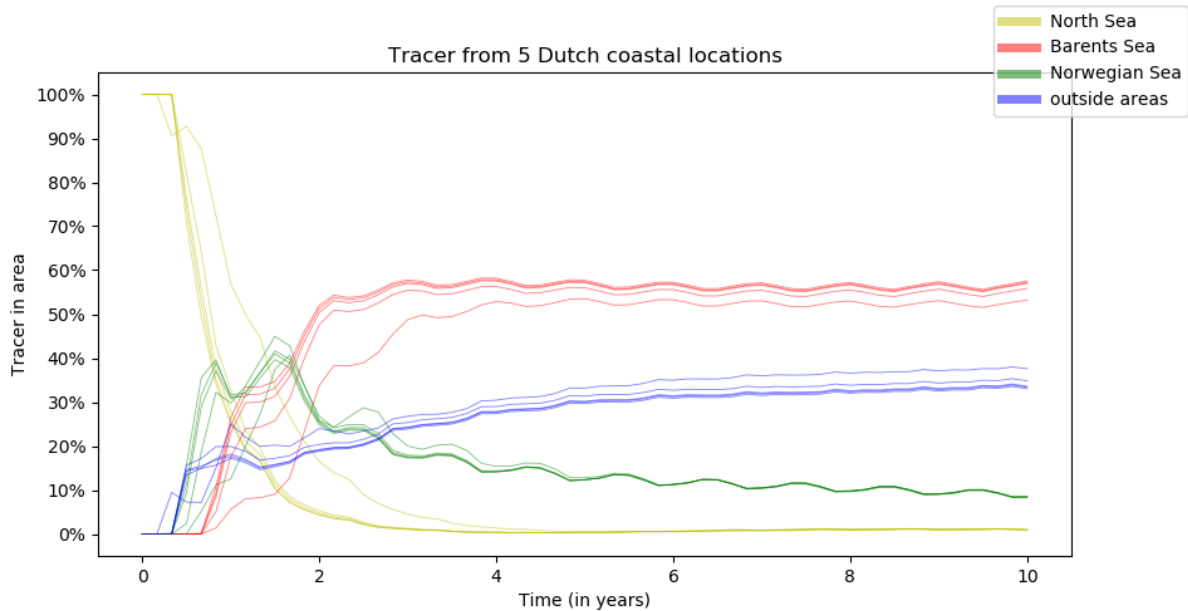
Figure 6: Tracer concentrations over time without beaching. For legibility of the graph, Kattegat is omitted as seperately plotted lines and is included in 'outside areas'. 'Outside areas' tracer is mostly found in Kattegat and Atlantic Ocean (16% and 4% respectively).

parameter to where the plastic ends up. In order to answer this question, plastic is released from five different release locations along the coast (see figure 4). This released tracer is advected for 10 years without any beaching taken into account, and its location over time is plotted in figure 6 for all five release points, corresponding to the areas labeled in figure 5. Since there are five release points, the graph has five lines for every area where plastic accumulates. As can be seen, there is some variance in tracer accumulation for the first three years depending on release location, but the lines converge towards similar values after this time. In these first three years, the only tracer release location that varies significantly from the others is the southernmost release point, which remains in the North Sea longer and enters the Barents Sea at a later point in time.

As can be seen from figure 6, most of the tracer released from the Dutch coast leaves the North Sea within two years and mostly travels through the Norwegian Sea to the Barents Sea and Kara Sea. The remainder of tracer mostly goes to the Skagerrak and Kattegat near Denmark and to the Atlantic Ocean (16 procent and 4 procent respectively, not shown in graph). In the Barents Sea and Kara Sea, tracer accumulation reaches 58% at its maximum.

Since there is very little difference in tracer pathways due to release location, from now on all experiments will have tracer input from all locations on the Dutch coast. These inputs will be scaled to the population density on the nearest shore (see table 1), since this has been assumed to be an accurate proxy for plastic disposal amounts in previous research [16] [1]. All inputs from now on will also happen in equal amounts during all timesteps for the first year, to mitigate seasonal variability. For more on this, see the Appendix.

Release coordinate	Adjacent province	Population density
(51N, 3E)	Zeeland	214
(52N, 4E)	Zuid-Holland	1287
(53N, 5E)	Noord-Holland and Friesland	$\frac{1046+194}{2}$
(53N, 6E)	Friesland	194
(53N, 7E)	Groningen	251

Table 1: Population density data (in inhabitants per km^2) used to scale tracer inputs from release locations shown in figure 5.

3.2   Beaching

Using the model described in the Method section, we now look at accumulation of tracer on shores. To get an overall impression of the locations of interest, we run a simulation of 10 years from the Dutch coast at a scaling factor of $s = 0.3$ and visualize the accumulation areas in figure 7. In this map we can see that there is some plastic accumulation on Greenland, the UK and the north coast of Russia, but the majority of plastic that ends on shore is accumulated on the Dutch, Norwegian and Danish shore. These areas with most plastic accumulation were also previously found to be areas of great plastic accumulation in the Lebreton et al. beaching simulation for the entire ocean, especially the points of relative high concentration on the (east-)Danish coast and one location on Nova Zemlya [5]. A more close-up plot of this area can be seen in figure 8, where we can identify the east coast of Denmark as the region where most plastic released from the Dutch shore ends up. This is presumably due to the circulatory trajectory of this area: any tracer that ends up in this area is likely to circle around in it and is unlikely to leave it again. Also, since the grid cells consist largely of small islands, jagged coastlines and bays, the area is highly fractional. To put this quantitavily: when excluding landpoints, the average beaching fraction $b_{avg} = 0.44$ for the area $54° \leq$ longitude $\leq 57.5°$ and $9° \leq$ latitude $\leq 12°$, in contrast to $b_{avg} = 0.03$ for the whole ocean.

As was mentioned before, there is little empirical evidence available for the proportion of input plastic that leaves the ocean by beaching. By varying the scaling factor of our model and looking at the effects on plastic accumulation, we can recalibrate our model to a scaling factor that realistically captures the beaching of plastic as more empirical data becomes available. In figure 9, the accumulation of plastic in the areas as defined in the previous section can be seen for various scaling factors. As expected, total amount of tracer beached increases with increasing scaling factor. Interestingly, some variance in proportion between the areas can be seen as well. When the scaling factor is higher, relatively more plastic washes ashore on beaches close to the point of release, such as on beaches adjacent to the North Sea and the Norwegian Sea. The amount of plastic that ends up on or near the Danish shore (the Kattegat area) appears to be similar irrespective of scaling factor, adding credibility to the hypothesis that the circular nature of the trajectories in this area play a major role in the accumulation of plastic on shores in this area.
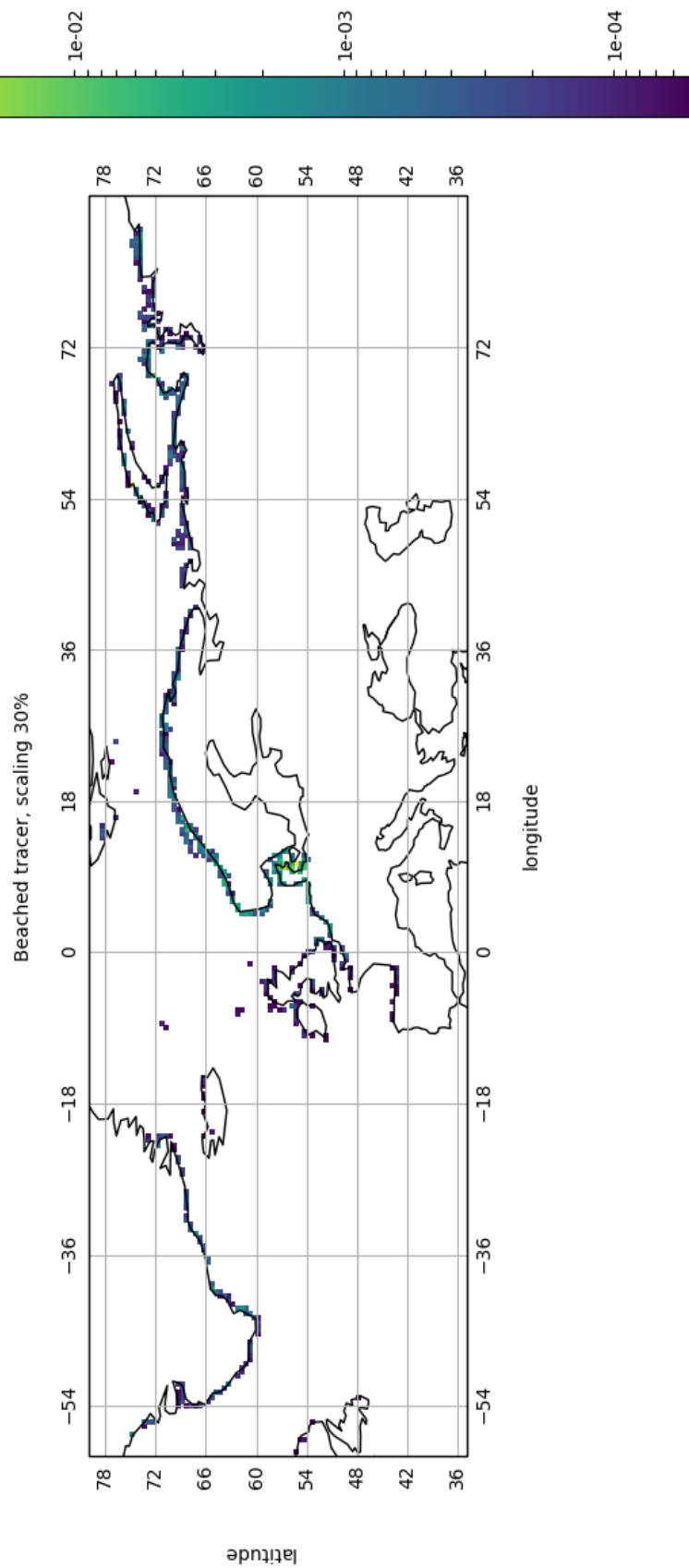
Figure 7: Map of all locations where at least 0.005% of released tracer stranded on beach. $s = 0.3$. The color scale is logarithmic.
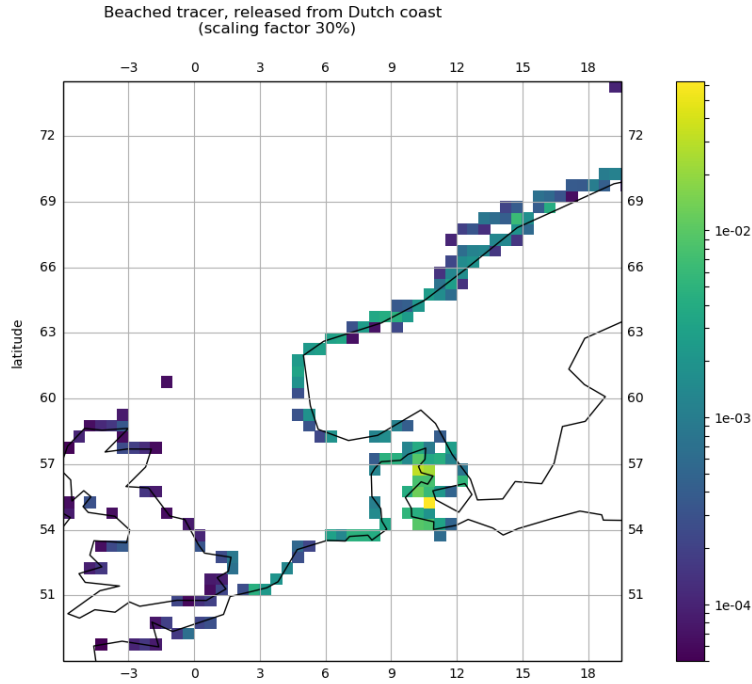
Figure 8: Close-up of North Sea area plastic accumulation (cf. figure 7). Scaling factor $s = 0.3$, the grid resolution is $dx = 0.5°$ and the color scale denotes the fraction of total released plastic that washed ashore per grid cell. The color scale is logarithmic.

Another relevant parameter we explore here is the model resolution. There are two reasons this parameter is relevant for our model. Firstly, the transit matrices will show different artificial dispersion effects depending on the model cell size [9]. Secondly, since the beaching model is based on data with a $0.1° \times 0.1°$ resolution, models with a finer resolution will use a coarser beaching grid (e.g. for $dx = 0.2°$, only four datapoints determine the beaching fraction for each cell). In figure 10, the differences in beached plastic are shown for fixed scaling factors $s = 0.05$ and $s = 0.3$. The differences are not as large as the variance in scaling factors, but there is a noticable increase in beaching when model grid size increases as well. This is likely the effect of our beaching model cell definitions, which will be further elaborated on in the Discussion section. Notably, the increase in accumulation is now mostly present in the regions where plastic ends up after four years of release, i.e. in the Barents Sea and Kattegat areas. It is possible this is the result of the longer time the plastic is circulating in these areas, as the tracer in this area drifts along these shores more frequently than in the North Sea and Norwegian Sea areas and the increased beaching effect of the larger model cells has more frequent contributions.
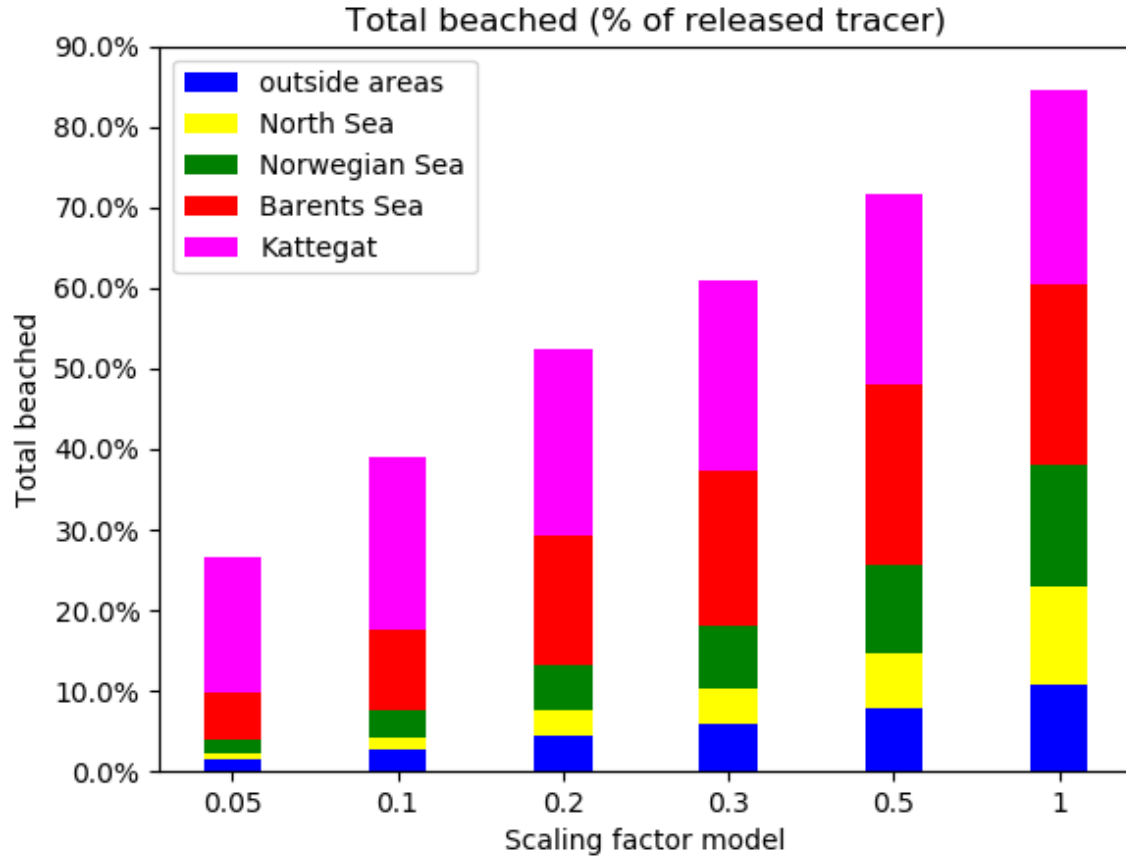
Figure 9: Amount of tracer beached in areas for various scaling factors after advection for 10 years. Resolution $dx = 0.5°$
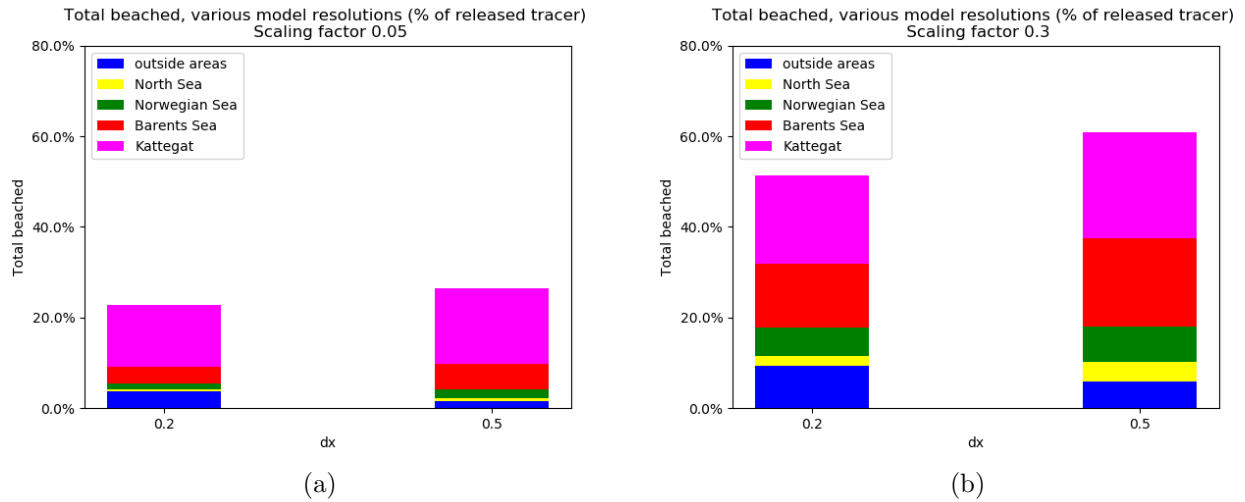

(a)

(b)

Figure 10: Plastic accumulation in areas for various model resolutions. Scaling factors are $s = 0.05$ and $s = 0.3$ respectively.

4   Discussion, outlook and conclusion

4.1   Discussion

One of the main issues with interpreting our results, is that there is little to no emperical data available on the amount of beached plastics related to their respective origin location. This has to do with the complexity of isolating the issue of beaching: it is time consuming and resource demanding to perform surveys on beaches to record the total amount of plastic, the origin of plastic recorded is hard to determine and it requires assumptions on the size and location of plastic inputs. One of the few extensive surveys available is a survey that was done on the Australian shore [3], but due to the number of assumptions - e.g. that all washed up plastic originated from Australia - it is not directly applicable for calibrating our model. Fortunately, research on the subject has increased in recent years, which will likely allow retro-active calibrating of the model as more data becomes available in the near future.

Another issue with the method is that the eddy resolving model data used to construct the transition matrices does not adequately reflect the complexity of the North Sea currents. As mentioned in the study by Masumoto et al. [7], non-hydrostatic processes and tidal movements are not included in the model data, which would be expected to be a significant factor in beaching, as these movements are important to the description of coastal areas. However, the buoy trajectories are subject to these movements and model data that does match the North Sea basin system accurately is being developed. As this becomes available, the model data used in this research can easily be swapped for newer, more accurate data sets. While the results in this paper are reliable to first order, they should be interpreted as exploratory instead of definitive. The results do give a coarse picture of accumulation zones for every origin location, allowing further research to be more precisely focused.

4.1.1   Beaching model

One of the flaws in our beaching model is that it does not take into account the shape of the coastline in a grid cell, only the amount of land in a grid cell. Consider for example two grid cells with equal beaching factors b, where one grid cell has the form of a bay and one grid cell has a straight line coast with a considerable inward land portion. It would be expected that the bay grid cell will have an increase in beaching compared to the straight line coast, and in a recent survey on debris beaching more litter was found on coastlines with a concave shape than on convex coastlines [3]. However, in its current configuration, the model will not show this. One way of solving this is creating a model where not only the portion of land in a grid cell is used as the beaching parameter, but also the tally of coasts adjacent to sea cells. The downside to this is that there are far more assumptions and choices to be made regarding this model. A few examples of this include the choice in proportional weighing of the amount of land to the amount of coastlines for the beaching factor b, more rounding errors due to grid definitions, the assumption whether diagonal coastlines should have any influence on the model, etcetera. As such, this model was not explored in this research, but it may be fruitful to take this into account for further research.
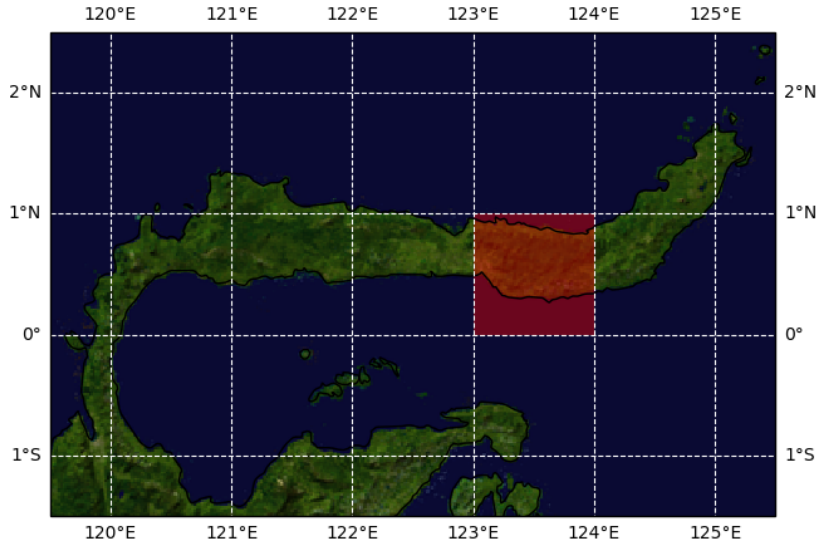
Figure 11: Example of a grid cell in Indonesia that has sea separated by land. In a beaching model, only the coastline adjacent to the sea where plastic tracer is should be considered in beaching, but the formulation of both beaching models proposed here cannot take this into consideration.

A factor that should not be overlooked in the beaching model is that when the resolution of the model used in this research is changed, is that the underlying elevation data on which the beaching model is based does not. This elevation dataset has a fixed resolution of $dx = 0.1°$, meaning that the value of b will become coarser when the model resolution is increased. E.g. for model resolution $dx = 1°$, $n_{totalcells} = 100$ and for $dx = 0.5°$, $n_{totalcells} = 25$, thus b increments with steps of 0.01 and 0.04 respectively. For $dx = 0.2°$, the total amount of datapoints involved in determining b would be $n_{totalcells} = 4$ with the current input data, which was deemed insufficient for realistic beaching effects in this paper. When increasing the resolution of the model further, beaching data with a higher resolution has to be implemented.

Both the model used in this research as well as the one proposed suffer from errors introduced by the assumption that the ocean is a Markov model. Consider the example model cell in figure 11 around Indonesia: tracer that flows through the cell on the north coast of the land will be subjected to a beaching influence from both the north and south coast, but the only relevant physical contribution to the beaching should be from the north coast. This problem is mitigated by increasing the model resolution, but remains an inherent problem of the modeling approach, because the approach ignores the previous location of tracer once it's in a cell [9]. Fortunately, the extreme example of a grid cell displayed in figure 11 does not occur in the region through which most Dutch plastic disperses and therefore this concern is largely negligible in this research, but it should be taken into account when this model is applied to different situations.

Further assumptions that were made in this model are that we do not account for other

sinks of plastic, such as animal ingestion of particles or sinking of plastic to ocean floors due to e.g. biofouling. Since there is little research done on this subject, it is hard to know how big this influence is on our results.

4.2   Confidence in results

One of the main shortcomings of interpreting this research is that no quantifiable values for confidence intervals are given, such as the standard deviation of results we consider comparable. This is the result of our inability to do statistically independent reruns of our simulation: when the simulation is repeated, the result will be exactly the same due to the deterministic nature of the transition matrices. The result of advecting the tracer distribution over time is a density field, instead of individual debris trajectories that would be comparable. One way of going around this problem is to perform the same experiment with a Monte Carlo simulation, where the transition matrices are used as chances for one debris particle to move from one grid box to another after one timestep, instead of using a diffuse tracer like we do now. This is similar to the method used in the 2011 van Sebille et al. paper [15].

Another option considered is taking the standard deviation over the difference density field in time for tracer fields we consider comparable. This is also not a viable option, due to the cyclical nature of the plastic trajectories. When comparing two pathways in time by taking a difference field, the assumption is made that the specific tracer concentrations of specific locations at specific times, are fundamentally different from a similar distribution in the same area if the specific concentrations, locations and times do not match, even though we know that the tracer mostly moves in cycles in a gyre.

Also, when we would take the difference density field over all locations that see tracer over time into account, we would see an inflated confidence due to most grid boxes considered having zero or near zero tracer in them. This is due to the fact that, while most particle tracer is in a relatively small area, small concentrations disperse throughout all of the ocean. These locations all over the world would play an excessive role in determining a standard deviation, which would lead to an artificially high claim of confidence.

Arguably the best way of providing a confidence interval would be with a bootstrapping method. Bootstrapping would entail rerunning the simulations for many times (usually in the thousands) with varying transit matrices constructed from randomly chosen subsets of the input trajectories used. These randomly chosen subsets would have the same number of crossings as our original matrices, thus providing a large sample of results with variance on which we can base our confidence assessment. Due to time constraints, this has not been performed for this research.

In short, there are simply too many degrees of freedom in the simulation to make an accurate assessment of how confident we are about these results at this time. Due to the exploratory nature of the research, this is not an insurmountable issue, but it should be taken into account when exploring the research question further.

4.3 Future research

Using a tracer based approach is apt for giving insight in the dispersion of plastic and the concentrations per area, but it is less applicable when the topic of research is the trajectories of individual plastic particles. Studying individual trajectories can give more insight in beaching behavior and plastic destinations, as conditionals can be applied to them (e.g. only consider plastic particles that move along the Norwegian coast and ignore all particles that move to the Kattegat). One way of doing this would be to perform a Monte Carlo simulation, using the transition matrices as the probability of a particle moving into a new cell after one timestep.

In a study published by Lumpkin et al. [6], an assessment has been made of the buoys used in this study that stopped transmitting a signal after some time, to distinguish the ones that stopped working due to faulty mechanics from the ones that ran aground. The study resulted in a statistical estimate of the proportion of these two explanations for buoy cessation. This data has not been used in this study, but could be incorporated in similar future studies to model realistic beaching mechanisms. In this study, grid cells in which buoys entered but did not leave again were given a reflective boundary condition and were not beached, to allow the model to not form a sink in this location artificially, since there is only a statistical estimate of which buoys would have stopped functioning for physical reasons and no definitive determination. For our aims here, this was sufficient, but future research could be improved upon by taking this into account.

Another interesting opportunity for future research is presented by an increase in observed buoy trajectories in the last five years, and the fact that these observations are ongoing and increasing. This new data unfortunately is so far largely located in already well-covered regions and adds little to sparsely covered regions such as the North Sea. However, it will potentially make results more accurate when these data are used and could also allow for raising the model resolution. In our research, we chose $dx = 0.5°$ as our main model resolution, since the higher resolution of $dx = 0.2°$ began to show artefacts in results. This may not be a problem anymore when the new data is also used. Note that when increasing the model resolution to $dx = 0.2°$, it is also necessary to find higher resolution data for the beaching model, as has been mentioned in the "Beaching model" subsection of this chapter.

Note that although scaling factors for the beaching model in this research did not exceed $s = 1$, there is no physical reason this could not be done in future research if it matches empirical evidence. However, when the scaling factor is raised above 1, grid cells that have a small proportion of sea will see all tracer beached that enters the cell. For instance, when the scaling factor is raised to $s = 1.25$, tracer in a grid cell with $b = 0.8$ will have a $p = 1$ chance of ending on shore.

4.4 Conclusion

In this study, we have used a transition matrix approach to simulate plastic pathways starting from the Dutch coast. We have seen that plastic from the Dutch coast mostly travels

northwards, where it splits in a small proportion going towards the Kattegat and a large proportion going along the Norwegian coast towards the Barents Sea and Kara Sea, where it ends bound in a gyre. We have seen that the variance between pathways starting from the north coast and those starting from the south coast of the Netherlands is small, and that differences between these pathways mostly occur in the first three years of plastic release in the sea. After these three years, there is no significant difference between the locations the plastic was released from. Similarly, while the timestep in which the plastic is released in the ocean matters in the first three years for the amount of plastic beached, the total amount of beaching after five years becomes similar regardless of the timestep in which the plastic was released.

Most plastic from the Netherlands that washes ashore ends up on the Danish coast, the Norwegian coast and the Dutch coast itself. The highest concentration of plastic accumulation happens on the east coast of Denmark. The scaling factor used in the model mostly influences the total amount of plastic beached, but does not change the relative ratio of plastic accumulation per area by much. The effects on proportion between these areas that can be noticed is that when the scaling factor is high, more beaching happens in regions closer to the origin of the plastic, and the absolute amount of plastic accumulation in the Kattegat seems to be constant regardless of the scaling factor. As more empirical evidence becomes available on the subject of beaching, retroactive scaling of the model can be done as a calibration measure, and our results can also suggest interesting areas for empirical surveying.

The effect of model resolution was also investigated. Larger grid cells were found to contribute to more overall beaching, but had little influence on the proportion of plastic accumulation between areas. The difference in beaching between these model resolutions can likely be partially explained by artificial dispersion inherent in Markov modeling of the ocean.

Future research should implement better input data for constructing transition matrices, such as the updated observational buoy data from the last few years, as well as model data that is more adequate in reflecting the dynamics of the North Sea. Possible future improvements of the model is to include coastal shapes into the beaching mechanisms as well, as opposed to only considering the fraction land and sea.

References

[1] CBS. Statline - regionale kerncijfers nederland, 2018. URL https://opendata.cbs.nl/statline/#/CBS/nl/dataset/70072ned/table?ts=1525115542068. Accessed: 2018-05-16.

[2] B. Cushman-Roisin and J.-M. Beckers. *Introduction to geophysical fluid dynamics: physical and numerical aspects*, volume 101. Academic Press, 2011.

[3] B. D. Hardesty, T. Lawson, T. van der Velde, M. Lansdell, and C. Wilcox. Estimating quantities and sources of marine debris at a continental scale. *Frontiers in Ecology and*

the Environment, 15(1):18–25. URL `https://esajournals.onlinelibrary.wiley.com/doi/abs/10.1002/fee.1447`.

[4] D. W. Laist. Impacts of marine debris: entanglement of marine life in marine debris including a comprehensive list of species with entanglement and ingestion records. In *Marine Debris*, pages 99–139. Springer, 1997.

[5] L. C. M. Lebreton, S. D. Greer, and J. C. Borrero. Numerical modelling of floating debris in the world's oceans. *Marine Pollution Bulletin*, 64:653–661, March 2012.

[6] R. Lumpkin, N. Maximenko, and M. Pazos. Evaluating where and why drifters die. *Journal of Atmospheric and Oceanic Technology*, 29(2):300–308, 2012. URL `https://doi.org/10.1175/JTECH-D-11-00100.1`.

[7] Y. Masumoto, H. Sasaki, T. Kagimoto, N. Komori, A. Ishida, Y. Sasai, T. Miyama, T. Motoi, H. Mitsudera, K. Takahashi, H. Sakuma, and T. Yamagata. A fifty-year eddy-resolving simulation of the world ocean - preliminary outcomes of ofes (ogcm for the earth simulator). *Journal of the Earth Simulator*, 1:35–56, January 2004.

[8] N. Maximenko, J. Hafner, and P. Niiler. Pathways of marine debris derived from trajectories of lagrangian drifters. *Marine Pollution Bulletin*, 65(1):51 – 62, 2012. URL `http://www.sciencedirect.com/science/article/pii/S0025326X11002189`.

[9] R. McAdam and E. van Sebille. Surface connectivity and interocean exchanges from drifter-based transition matrices. *Journal of Geophysical Research: Oceans*, 123:514–532, January 2018.

[10] NASA. Topography. URL `https://neo.sci.gsfc.nasa.gov/view.php?datasetId=SRTM_RAMP2_TOPO`.

[11] S. E. Pazan and P. Niiler. New global drifter data set available. *Eos, Transactions American Geophysical Union*, 85(2):17–17, 2004.

[12] P. Sherman and E. van Sebille. Modeling marine surface microplastic transport to assess optimal removal locations. *Environmental Research Letters*, 11(1):014006, 2016. URL `http://stacks.iop.org/1748-9326/11/i=1/a=014006`.

[13] U. G. Survey. Usgs products - gtopo30. URL `https://lta.cr.usgs.gov/citation`. Accessed: 2018-05-16.

[14] E. van Sebille. Adrift.org.au — a free, quick and easy tool to quantitatively study planktonic surface drift in the global ocean. *Journal of Experimental Marine Biology and Ecology*, 461:317 – 322, 2014.

[15] E. van Sebille, L. M. Beal, and W. E. Johns. Advective time scales of agulhas leakage to the north atlantic in surface drifter observations and the 3d ofes model. *Journal of Physical Oceanography*, 41(5):1026–1034, 2011. URL `https://journals.ametsoc.org/doi/abs/10.1175/2011JPO4602.1`.

[16] E. van Sebille, M. H. England, and G. Froyland. Origin, dynamics and evolution of ocean garbage patches from observed surface drifters. *Environmental Research Letters*, 7(4):044040, 2012.

[17] A. T. Williams, N. G. Rangel-Buitrago, G. Anfuso, O. Cervantes, and C. M. Botero. Litter impacts on scenery and tourism on the colombian north caribbean coast. *Tourism Management*, 55:209 – 224, 2016. URL `http://www.sciencedirect.com/science/article/pii/S0261517716300218`.

A   Appendix

A.1   Differences in beaching per release moment

If we find any significant differences between release moments, we would expect them to occur in the first few years since release. For this reason, a scaling factor of s = 1.0 was chosen, since this corresponds to the heaviest beaching effect and would magnify any differences between the release moments. Because of computational efficiency, the simulation for multiple release moments has been made on a $1° \times 1°$ grid.

In figure 12, the differences in beaching for different release moments can be seen. After a ten year period of advection (figure 12c), the differences between the total amount of beaching per area are all but non-existant, except for the release in timestep September-October, where less plastic beaches along the North Sea and more plastic beaches in areas other than the defined areas. However, when only advected for three years and five years (figure 12a and 12b respectively), there is a significant difference between beaching in these areas. For our purposes, we can interpret the difference between time release as negligible and thus use a release during the whole year for all other experiments in our research, where equal input is released into the ocean at every timestep during the first year. When working on smaller time scales, the differences can be relevant, so this should be taken into account in future research.

A.2   Differences in beaching between releasing plastic from coast and in open sea

As can be seen in figure 8, a significant amount of plastic accumulates on the shore from which it is released. This raises the question whether there is a noticeable difference in areas where plastic will end up between releasing plastic from the Dutch shore and releasing it further away in the North Sea, where it is not immediately subject to a neighboring coastline. To test this, an equal amount of tracer was released at the five open sea coordinates around 53N, 3E shown in figure 13, where all releases happened at $1\ \tau$ intervals, similarly to how tracer was released from the coast. Both release scenarios were then advected for ten years on a $dx = 0.5°$ grid with $s = 0.3$ and the results were plotted in figure 14a and 14b for the coast and open sea respectively. As can be seen, the results do not vary in a significant way, and only a handful of grid cells are visibly different. This justifies our release from coastal
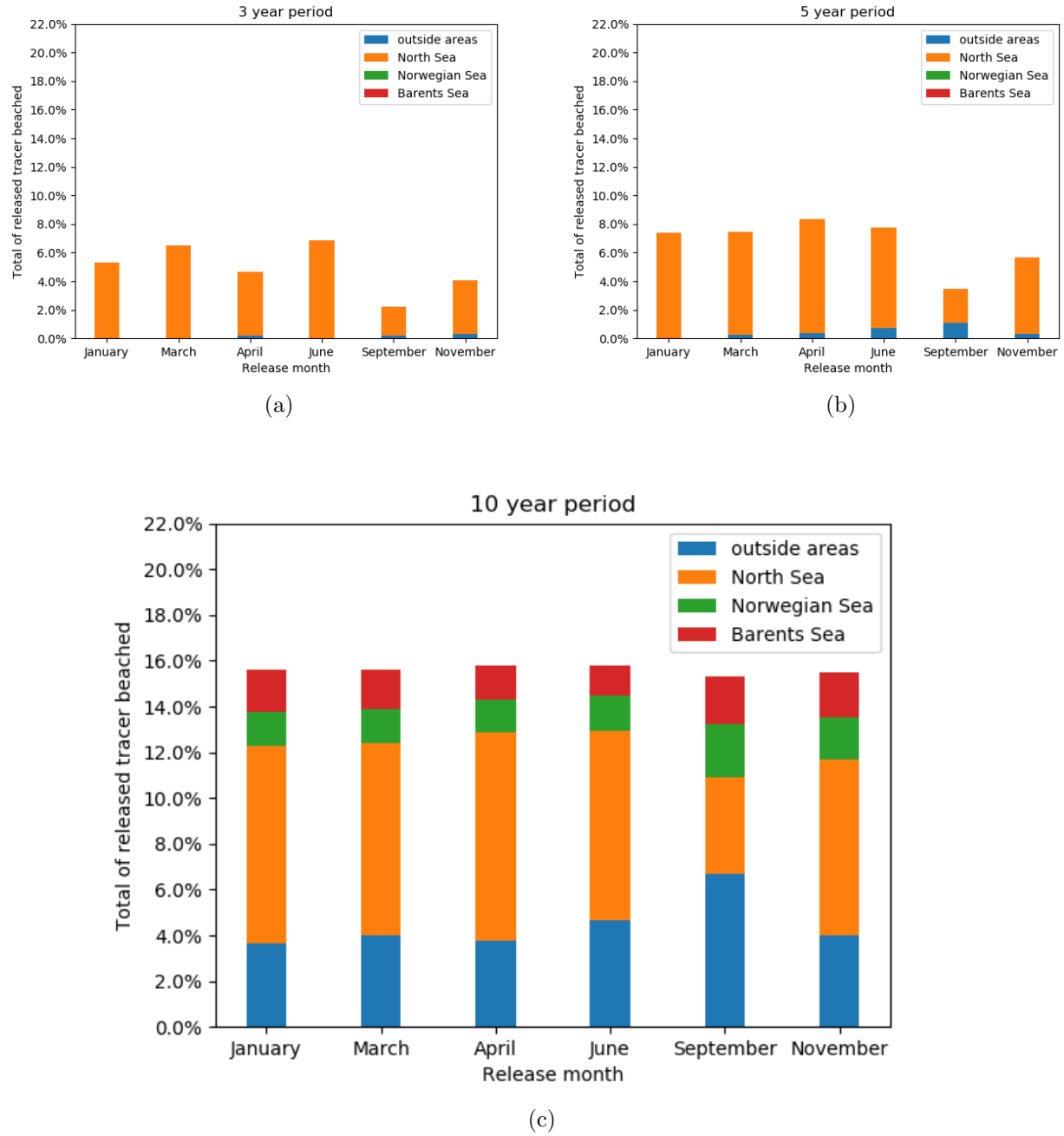
(a)

(b)

(c)

Figure 12: The amount of plastic beached after advection of three, five and ten years respectively. The scaling factor s = 1.0 and the grid resolution is $dx = 1°$
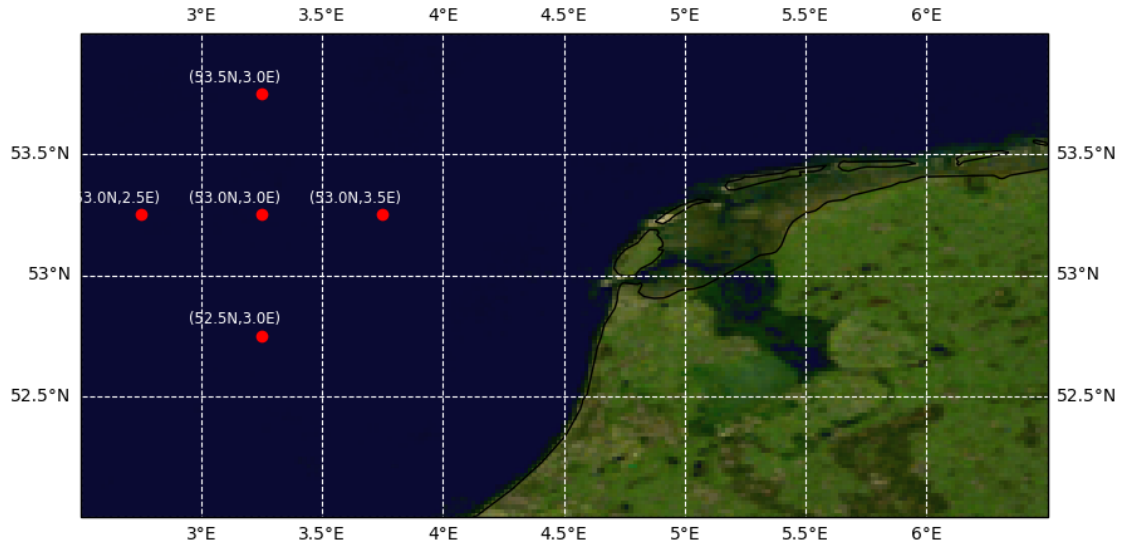
Figure 13: Locations of release in the North Sea. Input tracer concentrations are equal at all locations and the total amount of tracer released is equal to that released from the Dutch coast.
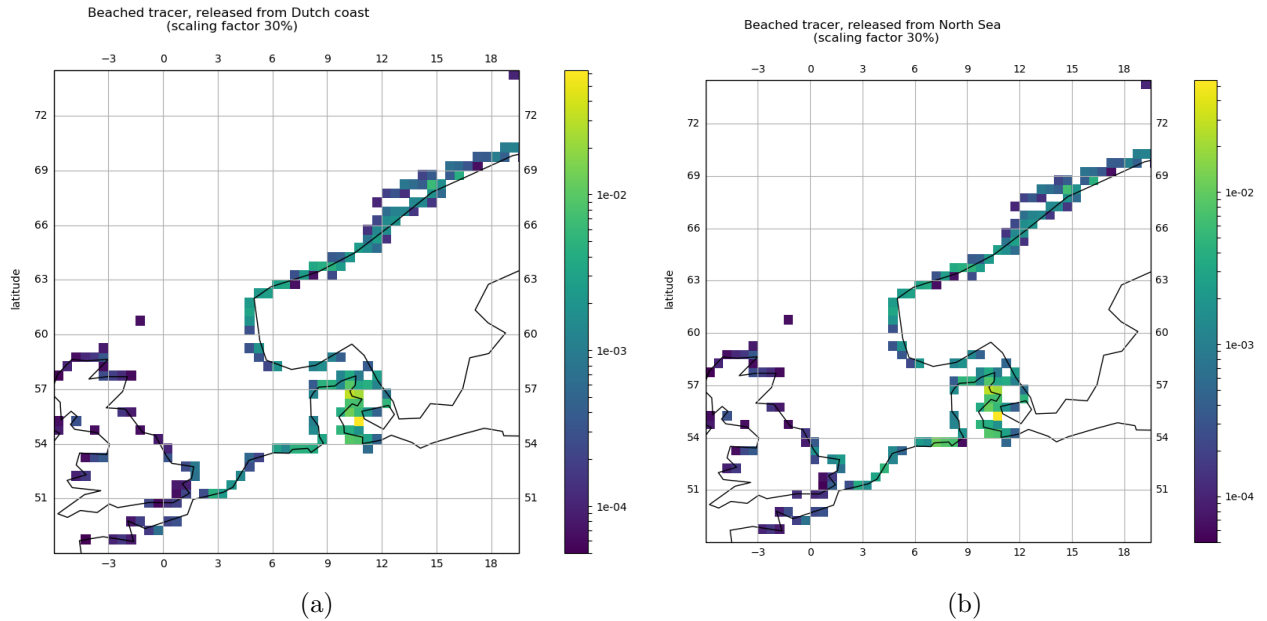

Figure 14: Map of plastic accumulation for release from coastal points and points in the open North Sea. The scaling factor is 30% and the grid resolution is $dx = 0.5°$. The color scale is plotted logarithmically.

grids in other experiments, as the release location does not seem to have a noticeable effect on beaching over longer periods of time.